HHS Public Access

Author manuscript

Eur J Pharmacol. Author manuscript; available in PMC 2022 April 05.

Published in final edited form as:

Eur J Pharmacol. 2021 April 05; 896: 173909. doi:10.1016/j.ejphar.2021.173909.

Membrane bound catechol-*O*-methytransferase is the dominant isoform for dopamine metabolism in PC12 cells and rat brain

Yupin Su[a,1], **Michael DePasquale**[a], **Gangling Liao**[a], **Ingrid Buchler**[a], **Gongliang Zhang**[a,2], **Spencer Byers**[a,3], **Gregory V. Carr**[a,b], **James Barrow**[a,b], **Huijun Wei**[a,b,4,*]

[a]Lieber Institute for Brain Development, Baltimore, MD, 21205, USA

[b]Department of Pharmacology, John Hopkins University, Baltimore, MD, 21205, USA

Abstract

Impaired dopamine activity in the dorsolateral prefrontal cortex (DLPFC) is thought to contribute to cognitive deficits in diseases such as schizophrenia, attention deficit hyperactivity disorder (ADHD) and traumatic brain injury. Catechol-*O*-methyltransfease (COMT) metabolizes dopamine and is an important regulator of dopamine signaling in the DLPFC. In mammalian species, two isoforms of COMT protein, membrane-bound COMT (MB-COMT) and soluble COMT (S-COMT), are encoded by one COMT gene and expressed widely. While S-COMT is thought to play a dominant role in the peripheral tissues, MB-COMT is suggested to have a greater role in dopamine metabolism in the brain. However, whether a selective inhibitor for MB-COMT may effectively block dopamine metabolism remains unknown. We generated a knockout of MB-COMT in PC12 cells using CRISPR-cas9 technology to evaluate the effect of both MB and S-COMT on dopamine metabolism. Deletion of MB-COMT in PC12 cells significantly decreased homovanillic acid (HVA), completely depleted 3-methyoxytyramine (3-MT), and significantly increased 3,4-dihydroxyphenylacetic acid (DOPAC) levels. Comparison of the effect of a MB-COMT selective inhibitor LI-1141 on dopamine metabolism in wild type and MB-COMT knockout PC12 cells allowed us to confirm the selectivity of LI-1141 with respect to MB-COMT in cells. Under conditions in which LI-1141 was shown to inhibit only MB-COMT but not S-COMT, it effectively changed dopamine metabolites similar to the effect induced by tolcapone, a non-selective COMT inhibitor, suggesting that selective inhibition of MB-COMT will be effective

[*]Corresponding author at Lieber Institute for Brain Development, Baltimore, MD, 21205, USA, 855 N. Wolfe St., Baltimore, MD 21205, USA, hwei11@jhmi.edu (H. Wei).

[1]Present address: 5 Research Ct, Rockville, MD 20850

[2]Present address: MedStar Health Research Institute, Baltimore, MD, 21218, USA

[3]Present address: Department of Biology, Boston University, Boston, MD, 02115, USA

[4]Present address: Department of Neurology, Brain Science Institute, John Hopkins University, 855 N. Wolfe St., Baltimore, MD 21205, USA

Yupin Su: Investigation; data curation **Michael DePasquale**: Investigation, data curation **Gangling Liao:** Investigation, data curation **Ingrid Buchler:** Writing - Review & Editing **Gongliang Zhang:** Methodology **Spencer Byers:** Investigation, data curation **Greg V. Carr:** Supervision, formal analysis **James Brrow**: Supervision, Writing - Review & Editing, funding acquisition **Huijun Wei:** Supervision, conceptualization, writing - Original Draft

Ethics statement on animal experimentation

All procedures involving animals were approved by the SoBran, Inc. Rangos Animal Care and Use Committee (Protocol #: LIE-011) and were in compliance with the *Guide for the Care and Use of Laboratory Animals.*

in blocking dopamine metabolism, providing an attractive therapeutic approach in improving cognition for patients.

Keywords

catechol-*O*-methyltransfease; dopamine; cognition

1. Introduction

Impaired dopamine activity in the DLPFC is thought to contribute to the cognitive deficits in schizophrenia, ADHD and traumatic brain injury (Lachman et al., 1996). COMT plays an important role in the metabolism of dopamine (Fig. 1). A single polymorphism in the human COMT gene leads to an amino acid change at position 158 from valine to methionine, resulting in less stable enzyme and slower dopamine metabolism (Chen et al., 2004). It has been shown that COMT Met158 is associated with improved performance in certain cognition-related tasks (Egan et al., 2001; Blasi et al., 2005), suggesting that inhibition of COMT activity in the brain may improve cognitive function.

The human and rat COMT orthologues contain a single gene with two promoters that direct the synthesis of two COMT mRNA isoforms (Tenhunen et al., 1993; Tenhunen et al., 1994). The shorter mRNA encodes S-COMT. The longer mRNA encodes for both MB-COMT and S-COMT through a leaky scanning mechanism of translational initiation (Tenhunen et al., 1993; Tenhunen et al., 1994), resulting in an additional 43 amino acids (aa) that contains a trans-membrane helix in the N-terminus of rat MB-COMT (Ulmanen et al., 1997). Western blot analysis in various human tissues showed that MB-COMT accounts for less than 26% of total COMT proteins in peripheral tissues such as liver, adrenal, kidney and duodenum, but it accounts for 70% of total COMT protein in the brain (Tenhunen et al., 1994). MB-COMT (Km=3.3μM) also was found to have higher affinity for dopamine than S-COMT (Km=278μM), therefore, MB-COMT is speculated to be the dominant enzyme for dopamine metabolism in the brain (Rivett & Roth, 1982; Roth, 1992). Inhibition of COMT activity has been shown to be associated with dyskinesia, tachycardia, diarrhea, orthostatic hypotension and chronic pain (Ciszek et al., 2016; Ferreira et al., 2019; Salamon et al., 2019), hypothesized to be due to the inhibition of the peripheral COMT activity. Therefore, selective inhibition of MB-COMT may provide efficacy in improving cognition while lowering the potential adverse side effects associated with S-COMT inhibition in the peripheral tissues.

MB-COMT specific inhibition with small molecules has been reported and shown to induce changes in the levels of dopamine metabolites (Robinson et al., 2012; Buchler et al., 2018; Ernst et al., 2019). However, many of these MB-COMT selective inhibitors are expected to partially inhibit S-COMT in the brain (Robinson et al., 2012; Buchler et al., 2018; Ernst et al., 2019). In addition, it is possible that the isoform selective inhibition is an artifact arising from different *in vitro* enzymatic assay conditions, including different substrates, and conditions with or without membrane and detergent. Therefore, whether inhibition of MB-

COMT alone will be effective in changing the metabolism of dopamine in the brain requires further study.

We have previously demonstrated that PC12 cells, a rat adrenal pheochromocytoma-derived cell line, express all key regulators for dopaminergic function, including MB-COMT and S-COMT (Zhang et al., 2019). In this study, we investigated the role of MB-COMT on dopamine metabolism in PC12 cells by deletion of MB-COMT using CRISPR-cas9 technology or specifically inhibiting MB-COMT activity using MB-COMT selective inhibitor.

2. Materials and Methods

2.1. Cell Culture and Media

PC12 cells were obtained from the American Type Culture Collection (Manassas, VA, USA; Product #: CRL-1721) and cultured in DMEM (Gibco/ThermoFisher Scientific; Product #: 31600–034) supplemented with 10% horse serum (Gibco/ThermoFisher Scientific; Product #: 16050–122), 5% fetal bovine serum (HyClone/ThermoFisher Scientific; Product #: SH30071.03), 1% penicillin streptomycin (Gibco/ThermoFisher Scientific; Product #: 15070–063) in a humidified incubator containing 5% CO_2 at 37 °C. The maximal cell passage number was 15 to prevent change in cellular function.

2.2. MB-COMT knockout in PC12 cells by CRISPR-Cas9

MB-COMT gene knockout on PC-12 cell was performed using CRISPR gene editing techniques. Three guide RNAs (gRNA-1: CTCCTGCTCTTGCGACACCT, gRNA-2: CCCAATGAGACTGCAGCCAA, and gRNA-3: AGCCCAGGTGTCGCAAGAGC) were designed targeting in the region between the start codon of S-COMT and MB-COMT. Guide RNA constructs were cloned into pSpCas9 BB-2A-Puro (PX459) v2.0 plasmid (GenScript, USA), and 1 μg of plasmid DNA was transfected into PC-12 cells on 6-well plate using Lipofectamine 2000 (Invitrogen, USA). Puromycin (1mg/ml) was added at 24 h post transfection to kill non-transfected cells. After 24 h incubation, cultural medium was replaced with puromycin-free medium and kept culturing until cells were grown. COMT gene was amplified with PCR (forward primer: TCCTCTACACAGGACTCCGG, reverse primer: GCTCCCCATTTCTAGGCTGT), and indels were analyzed with GeneArt genomic cleavage detection kit (Invitrogen, USA). Single colony selection was performed with limited dilution, about 100 cells were seeded onto a 96-well plate, incubated for one week. Single colonies were further grown in a 24-well plate for 7 to 10 days. MB-COMT DNA from each clone was amplified by PCR. The sequences were determined by Sanger sequencing using the PCR primers. The Inference of CRISPR Edits (ICE) scores were calculated using CRISPR edits software by Synthego (ice.synthego.com) to confirm the Indel and gene editing proficiency. MB-COMT protein knockout was confirmed with western blot using anti-COMT antibody (BD-611970, BD Bioscience, USA).

2.3. Soluble and membrane fraction preparation:

100,000 cells were harvested and extracted with membrane solution (15 mM Tris, pH7.5, 1 mM EGTA, 0.3 mM EDTA, 2 mM $MgCl_2$, PIC cocktail) with 2 cycles of freeze and thaw,

then treated with DNase I for 10 min at RT. After 20 min centrifugation at 13,600g, supernatant (S, soluble fraction) and pellet (M, membrane fraction) proteins were analyzed with 4–20% SDS-PAGE and western blot for COMT protein.

2.4. *In vitro* COMT enzyme activity assay

COMT activity assay were performed using the MTase Glo methyltransferase assay (Promega, Madison, WI, USA) as described previously (Zhang et al., 2019). Specifically, assays were carried out in Corning low volume 384-well white flat-bottom polystyrene NBS microplates with a final volume of 5 μl containing approximately 4 ng of human MB-COMT or 1 ng of human S-COMT as estimated by the Bradford Lowry method from the membrane homogenate. All reactions contained 20 μM high purity S-adenosyl methionine (SAM, Cisbio, Bedford, MA, USA) in COMT assay buffer (50 mM Tris, 5–10 mM $MgCl_2$, 2.5 mM DTT, pH 6.9). For MB-COMT, the catechol substrate was 7 μM norepinephrine (MilliporeSigma, St. Louis, MO, USA) and for S-COMT the substrate was 10 μM 7,8-dihydroxy-4-methylcoumarin (MilliporeSigma, St. Louis, MO, USA). Reactions were performed in a 37 °C incubator for 1 h. The plate was removed from the incubator and allowed to cool to room temperature for 15 min. MTase reagent A (Promega) was first diluted 1:5 into RO water, and 1 μl was then added to the well. The plate was spun down, shaken, and allowed to incubate for 30 min at room temperature avoiding light. Then 5 μl of MTase reagent B (Promega) were added to all of the wells. The plate was spun down, shaken, and allowed to incubate for 30 min at room temperature avoiding light. Luminescence was detected with a Tecan Infinite M100 Pro plate reader.

2.5. PC12 cells assay for dopamine metabolites

The PC12 cells assay for dopamine metabolites were performed as described previously (Zhang et al., 2019). Cells were plated at a density of 5×10^4 cells/well in 96-well plate. Inhibitor stock solution or DMSO were diluted in culture medium, then added to corresponding well immediately after cell plating. After 24 h incubation, the culture media was collected for analysis of DA and metabolites. All samples were stored at −80 °C before analysis. The LC-MS measurement for 3-MT, HVA and DOPAC were performed as described previously (Zhang et al., 2019).

2.6. Measurement of HVA and DOPAC in the cerebrospinal CSF

On the day of testing, Male CD® (Strain code: 001; Sprague Dawley) IGS rats (8–11 weeks old; Charles River Laboratories, Wilmington, MA, USA) were transferred to a holding room and weighed. After an hour acclimation period, rats received an oral dose of either vehicle (0.1% Tween80, 0.1% 1510 silicone antifoam, 1% methylcellulose 400c/p in water), LI-1141 (10 mg/kg), or tolcapone (15mg/kg dosed ip). Four hours following vehicle or drug administration, rats were moved to a separate procedure room where they were anaesthetized via isoflurane. Once the rats were determined to be unresponsive, their heads were shaved using electric clippers. The rats were positioned in a stereotaxic frame, with their heads pointed down at a 45-degree angle. To collect cerebrospinal fluid (CSF), previously published protocols (Nirogi et al., 2009; Mahat et al., 2012) were adapted. Briefly, a 23-gauge needle, connected via PE50 tubing to a collection syringe, was used to access the cisterna magna. Slight negative pressure was used to ensure the CSF flowed evenly. The

CSF was collected in previously chilled (dry ice) Eppendorf tubes containing 0.05M perchloric acid (4:1 CSF:perchloric acid ratio). The tubes were put back on dry ice until the end of the procedure. CSF samples with visible blood contamination were not used in subsequent bioanalytical analyses. Next, the chest cavity was opened, and blood was collected by cardiac puncture. The blood was collected in Lithium-Heparin 1.3 ml microtubes (Sarstadt, Numbrecht, Germany) and stored on ice. Blood was then centrifuged at 2000 g at 4°C for 10 min to separate the plasma. Plasma was then transferred into Thermo Scientific Matrix tubes (Thermo Fisher Scientific, Waltham, MA, USA) for storage. CSF and plasma were stored at −80°C until analysis. DA metabolite and COMT inhibitor concentrations were measured by LC-MS/MS as previously described (Buchler et al., 2018).

2.7. Data analysis

All data represent three separate experiments with each data point from each experiment representing the average of two separate wells. All statistical tests were conducted using Prism 9 (GraphPad Software, Inc., San Diego, CA, USA). $p < 0.05$ was considered statistically significant.

3. Results:

3.1. Selectively knockout MB-COMT in PC12 cells using CRISPR-cas9 technology

To selectively knockout MB-COMT in PC12 cells, we designed three different gRNAs targeting the region between the MB-COMT and S-COMT ATG translation initiation codons (Fig. 2A). After transfection and single colony selection, the genomic DNA region containing the CRISPR targeting sites in the COMT gene was amplified by PCR and sequenced. Because PC12 cells aggregate together easily, a colony obtained after colony selection may arise from a mixture of cells with different COMT gene mutations. Using the sequence chromatogram from the wild type cells as a reference, the sequence chromatograms from different colonies enabled us to calculate the inference of CRISPR edits (ICE) scores using a CRISPR edits software (ice.synthego.com). Colonies arising from a single cell are expected to have an ICE score near 100% derived from either 1 or 2 DNA sequences. To avoid misinterpretation resulting from potential off-target mutations from CRISPR, we chose several colonies with different mutations in the COMT gene obtained from different gRNAs for further analysis. For example, colony #1was obtained from gRNA-1 and has an insertion of an adenine nucleotide (nt) after the 62 nt downstream of the MB-COMT start codon with an ICE score of 99%, suggesting a common insertion on both copies of COMT genes (Fig. 2B). This insertion leads to a frame shift in MB-COMT starting at 21^{th} amino acid (aa) with a premature stop at 32^{th} aa. Colony #2 was obtained from gRNA-2 and has a deletion at the 10 nt downstream of the MB-COMT start codon on both copies of COMT genes. This deletion leads to a frame shift in MB-COMT starting at 4^{th} aa with a premature stop at 26^{th} aa. In addition, colony #3 was obtained from gRNA-3. This colony is heterozygous with only one copy of the COMT gene mutated while the other copy of COMT gene remains as a wild type with an ICE score of 49%. The mutation in the COMT gene has a deletion of two nucleotides (53 nt and 54 nt downstream of MB-COMT start codon), resulting a frame shift from MB-COMT starting at 22^{th} aa with a premature stop at 31^{th} aa.

To determine the effect of these mutations on MB-COMT and S-COMT expression, a membrane fraction and a soluble fraction of cells from these colonies were prepared. Western blot analysis confirmed that there is no detectable MB-COMT protein in colonies #1 and #2, and colony #3 has about 50% decrease in MB-COMT expression (Fig. 2C), consistent with our prediction from DNA sequencing results. Because the DNA region between the MB-COMT and S-COMT ATG translation initiation codons overlaps with the promoter region for S-COMT mRNA expression (Tenhunen, 1996), a mutation in this region may change the expression level of S-COMT protein by changing the mRNA level of S-COMT. However, we did not detect any change in S-COMT protein levels in any of these colonies. Therefore, we successfully knocked out MB-COMT without affecting the S-COMT expression.

3.2. Effect of MB-COMT deletion on dopamine metabolism in PC12 cells.

To determine the effect of MB-COMT deletion on dopamine metabolism, we compared dopamine metabolites in the wild type PC12 cells and various MB-COMT deletion colonies using an assay previously described (Zhang et al., 2019). 3-MT was below our limit of quantitation in all colonies with complete MB-COMT deletion, whereas heterozygous deletion of MB-COMT in the colony #3 decreased 3-MT by 80% (Fig. 3A). In general, the steady state concentration of 3-MT is low in PC12 cells and is only about 10 times our minimum detection level. Therefore, it is impossible to differentiate a complete inhibition from 90% inhibition of 3-MT. To further investigate whether S-COMT plays any role in 3-MT production, we treated cells with the MAO inhibitor pargyline to inhibit the metabolism of 3-MT. Treatment of pargyline at 0.1 μM increased the concentration of 3-MT level for more than 75% in the wild type PC12 cells, however, there was still no detectable 3-MT in the MB-COMT knockout cells even in the presence of pargyline, suggesting that MB-COMT accounts at least 94% of 3-MT production (Fig. 3B). This is consistent with the idea that 3-MT is entirely produced from dopamine by MB-COMT (Parkkila & Viitala, 2020).

In the heterozygous MB-COMT knockout cells, HVA concentrations are about 43% of those measured in wild type cells. Complete deletion of MB-COMT further lowered HVA concentration to approximately 25–28% of wild type in different colonies (Fig. 3C). This HVA level in the MB-COMT knockout cells is still 2.5 to 3 times its minimum detection level. We previously showed that complete inhibition of both S-COMT and MB-COMT by tolcapone decreased HVA to undetectable levels in wild type PC12 cells (Zhang et al., 2019). Together, these results suggest that S-COMT is also involved in the conversion of DOPAC to HVA in PC12 cells.

Deletion of MB-COMT was found to increase DOPAC (Fig. 3D). But the increase of DOPAC varied significantly in different colonies with a range of 60% to 250%. However, we did not detect accumulation of DOPAC levels in the cells with MB-COMT heterozygous knockout, suggesting that S-COMT and approximately half of endogenous MB-COMT found in wild type cells is enough to maintain the steady state of DOPAC in PC12 cells.

3.3. Effect of COMT inhibitors on dopamine metabolism in MB-COMT deletion cells.

We previously identified several compounds that are highly selective in inhibiting MB-COMT (Buchler et al., 2018; Ernst et al., 2019). LI-1141 is a very potent inhibitor against MB-COMT with an IC_{50} of 29 nM, but weakly inhibits S-COMT (IC_{50}=48,238 nM) in the *in vitro* enzymatic assay (Fig. 4). We therefore compared the effects of LI-1141 on dopamine metabolism in wild type and MB-COMT knockout PC12 cells. Treatment of wild type PC12 cells with 1 μM LI-1141 completely blocks 3-MT accumulation (Fig. 5A), an effect similar to that of MB-COMT deletion. In addition, treatment of the wild type PC12 cells with 1 μM LI-1141 decreased HVA levels approximately 75% (Fig. 5B), which is similar to the baseline levels of HVA in MB-COMT knockout cells in Fig. 3C. LI-1141 at 10 μM further decreased HVA to below the minimum detection level. This effect of complete inhibition of HVA production is similar to the effect by tolcapone, suggesting that LI-1141 also inhibits S-COMT in PC12 cells at 10 μM, an unexpected result given the in vitro IC_{50} from the enzyme assay. In addition, 1 μM LI-1141 also increased DOPAC levels about 70%. Increasing concentrations of LI-1141 to 10 μM did not significantly increase DOPAC levels further in the wild type PC12 cells (Fig. 5C).

To determine whether the effect of LI-1141 on dopamine metabolism is dependent on MB-COMT, we determined the effect of LI-1141 in MB-COMT deletion cells. LI-1141 at 1 μM significantly decreased HVA and increased DOPAC levels in the heterozygous knockout cells, but additional decrease the HVA level or increase the DOPAC level in the MB-COMT homozygous knockout cells was not observed. This suggests that this compound affects dopamine metabolism through MB-COMT at 1 μM (Fig. 5B and 5C). At 10 μM, LI-1141 did not significantly continue to increase DOPAC levels in MB-COMT homozygous knockout cells, but slightly decreased HVA to below the minimum detection level, consistent with inhibition of S-COMT at higher concentrations of inhibitor. Together, these data suggest that LI-1141 at 1 μM is highly selective against MB-COMT with minimum inhibition of S-COMT.

3.4. Effect of MB-COMT selective inhibitors on dopamine metabolism in the cerebrospinal fluid (CSF) in rats

Because PC12 cells are not neuronal cells, we wanted to confirm the effect of MB-COMT inhibition seen in PC12 cells in brain. Although free levels of dopamine are very low in CSF, the CSF dopamine metabolites HVA and DOPAC have been used historically to access central dopaminergic function (LeWitt, 1993). After single administration of LI-1141 (100 mg/kg, PO) drug concentrations were measured to be 289 nM in the brain and 56 nM in the CSF 4 h post dose. Because LI-1141 at lower than 1 μM is not expected to inhibit S-COMT, the effect of LI-1141 should be reliant on MB-COMT inhibition. The HVA level in the CSF of rats decreased by approximately 45% (t_{11} = 4.765, P = 0.0006) (Fig. 6A) and the DOPAC level increased to approximately 234% of the vehicle-treated group (t_{11} = 6.854, P < 0.0001) (Fig. 6B). As a comparison, intraperitoneal injection of 15 mg/kg of tolcapone decreased HVA by approximately 72% (t_{13} = 13.09, P < 0.0001) (Fig. 6C) and increased DOPAC to approximately 301% of the vehicle-treated group (t_{13} = 9.866, P < 0.0001) (Fig. 6D) when measured 4 h post dose (3.8 μM tolcapone plasma concentration). Therefore, selective inhibition of MB-COMT alone can effectively block dopamine metabolism in the brain

similar to inhibition of both MB-COMT and S-COMT, further supporting the hypothesis that pharmacologic inhibitors selectively inhibiting MB-COMT may be an effective therapeutic approach to improve the cognitive function.

4. Discussion

MB-COMT and S-COMT are identical in their catalytic domain and the only difference between the two isoforms of enzyme lies on the extra 43aa that includes the membrane anchoring domain at the N-terminal of MB-COMT. We recently identified many COMT inhibitors that are selective for MB-COMT (Ernst et al., 2019). It has been suggested that the transmembrane helix and linker segment of a membrane anchor protein may orient the position of the catalytic domain with respect to the membrane (Monk et al., 2014), which may lead to substrate preference for different isoforms of COMT (Parkkila & Viitala, 2020). A compound may also partition in the membrane and selectively inhibit MB-COMT (Parkkila & Viitala, 2020). In addition, binding of COMT to its cofactor *S*-adenosylmethionine (SAM) has been proposed to induce a conformational change that drives the catalytic surface of the protein to the membrane surface, thereby providing another mechanism for obtaining selective MB-COMT inhibition (Magarkar et al., 2018). On the other hand, it is also possible that the isoform specificity is an artifact resulted from the different assay conditions in *in vitro* enzymatic assays. Generation of MB-COMT knockout in PC12 cells enabled us to definitely answer whether these inhibitors are indeed MB-COMT selective. Because the MB-COMT and S-COMT are expressed from the same mRNA, degradation of mRNA by siRNA would not be applicable for the purpose of specifically knocking down MB-COMT while leaving S-COMT unaffected. We used CRISPR-cas9 to generate several different colonies with different mutations in the COMT gene using three different gRNAs. All of the mutations we identified have a premature stop codon within the 43aa membrane anchoring domain of MB-COMT, and the complete deletion of MB-COMT was confirmed by Western blot. Because the DNA region between the MB-COMT and S-COMT ATG translation initiation codons overlaps with the proximal P1 promoter region important for S-COMT mRNA expression (Tenhunen, 1996), a mutation in this region may change the expression level of S-COMT protein by changing the mRNA level of S-COMT. However, we did not detect any change in S-COMT protein levels in any of these colonies. This may due to a small insertion or deletion in this region did not significantly affect the promoter activity and expression of the shorter mRNA encoding for S-COMT expression remains the same. Alternatively, PC12 cells may only express the longer mRNA transcript encoding for both MB-COMT and S-COMT, and the mutation in the region upstream of the translation initiation codon of S-COMT did not affect its translation.

Here we present data using colonies with homozygous mutations with the same deletion or insertion in both copies of COMT gene. Similar results were obtained using other colonies with both copies of MB-COMT gene deleted but have different insertion or deletion in different copies of the gene (data not shown). Although we did not perform whole genome sequencing and cannot rule out that different colonies may have other off target mutations, it is very unlikely that these three different gRNAs lead to same off-target mutations, resulting in the consistent effects on dopamine metabolism.

Deletion of MB-COMT completely depleted the metabolite 3-MT in PC12 cells, suggesting that MB-COMT is the primary isoform for directly metabolizing dopamine. At physiological pH, dopamine is positively charged and can interact dominantly with negative charges on phospholipids in the membrane, which may explain why the membrane bound isoform MB-COMT is solely responsible for dopamine methylation. Deletion of MB-COMT decreases HVA by 75%, and inhibition of both S-COMT and MB-COMT can further deplete the residual HVA to undetectable levels in the cells, suggesting that S-COMT accounts for those residual 25% HVA production in MB-COMT knockout cells. Because DOPAC levels, which is the substrate for S-COMT, are significantly higher in MB-COMT knockout cells, the relative contribution of S-COMT for HVA production in the wild type PC12 cells may be even lower.

Treatment of wild type cells with LI-1141 at 1 μM resulted in a similar dopamine metabolite profile to that seen in the MB-COMT knockout cells. In addition, LI-1141 at 1 μM did not further change HVA or DOPAC levels in the MB-COMT knockout, suggesting that the effect of this compound at 1 μM on dopamine metabolites is completely dependent on MB-COMT. Increasing the compound concentration to 10 μM resulted in a further decrease in HVA to undetectable level, which is similar to the effect of tolcapone, suggesting that LI-1141 at 10 μM also significantly inhibits S-COMT in the cells. Such effect is not consistent with the IC_{50} of 48 μM obtained from *in vitro* assay, suggesting the selectivity achieved from *in vitro* IC_{50} analysis may be overestimated.

The PC12 cell line was derived from rat adrenal pheochromaocytoma. It expresses all key regulators for dopaminergic function and has been extensively characterized in dopamine synthesis and release (Westerink & Ewing, 2008). Treatment of wild type PC12 cells with MB-COMT specific inhibitors displayed similar profile in dopamine metabolism to MB-COMT knockout cells. Furthermore, we observed MB-COMT specific inhibitor display similar profile in the dopamine metabolism in PC12 and in the rat brain. Such correlation suggests that evaluation of the effect of a COMT inhibitor in PC12 cells may serve as a surrogate for predicting its effect *in vivo,* which will significantly increase the speed and lower the cost for developing a COMT inhibitor for improving cognition.

5. Conclusions:

We have successfully knocked out MB-COMT specifically in PC12 cells and demonstrated that MB-COMT plays a dominant role in the dopamine metabolism in PC12 cells and rat brain. We also demonstrated that LI-1141 at 1 μM inhibits MB-COMT but not S-COMT in our cell-based assay. By measuring the free drug concentration in the brain, we were able to show that LI-1141 achieved similar effects on dopamine metabolites to tolcapone treatment. This provides direct evidence that pharmacological inhibitor selective for MB-COMT may limit S-COMT peripheral side effects and be effective for the treatment of cognitive defects associated with schizophrenia, head trauma and ADHD.

Acknowledgments

Funding:

This work was supported by the National Institutes of Health [R01 MH107126] and the Lieber Institute for Brain Development.

References:

Blasi G, Mattay VS, Bertolino A, Elvevag B, Callicott JH, Das S, Kolachana BS, Egan MF, Goldberg TE & Weinberger DR (2005) Effect of catechol-O-methyltransferase val158met genotype on attentional control. J Neurosci, 25, 5038–5045 DOI: 10.1523/JNEUROSCI.0476-05.2005 [PubMed: 15901785]

Buchler I, Akuma D, Au V, Carr G, de Leon P, DePasquale M, Ernst G, Huang Y, Kimos M, Kolobova A, Poslusney M, Wei H, Swinnen D, Montel F, Moureau F, Jigorel E, Schulze MED, Wood M & Barrow JC (2018) Optimization of 8-Hydroxyquinolines as Inhibitors of Catechol O-Methyltransferase. J Med Chem, 61, 9647–9665 DOI: 10.1021/acs.jmedchem.8b01126 [PubMed: 30272964]

Chen J, Lipska BK, Halim N, Ma QD, Matsumoto M, Melhem S, Kolachana BS, Hyde TM, Herman MM, Apud J, Egan MF, Kleinman JE & Weinberger DR (2004) Functional analysis of genetic variation in catechol-O-methyltransferase (COMT): effects on mRNA, protein, and enzyme activity in postmortem human brain. Am J Hum Genet, 75, 807–821 DOI: 10.1086/425589 [PubMed: 15457404]

Ciszek BP, O'Buckley SC & Nackley AG (2016) Persistent Catechol-O-methyltransferase-dependent Pain Is Initiated by Peripheral beta-Adrenergic Receptors. Anesthesiology, 124, 1122–1135 DOI: 10.1097/ALN.0000000000001070 [PubMed: 26950706]

Egan MF, Goldberg TE, Kolachana BS, Callicott JH, Mazzanti CM, Straub RE, Goldman D & Weinberger DR (2001) Effect of COMT Val108/158 Met genotype on frontal lobe function and risk for schizophrenia. Proc Natl Acad Sci U S A, 98, 6917–6922 DOI: 10.1073/pnas.111134598 [PubMed: 11381111]

Ernst G, Akuma D, Au V, Buchler IP, Byers S, Carr GV, Defays S, de Leon P, Demaude T, DePasquale M, Durieu V, Huang Y, Jigorel E, Kimos M, Kolobova A, Montel F, Moureau F, Poslusney M, Swinnen D, Vandergeten MC, Van Houtvin N, Wei H, White N, Wood M & Barrow JC (2019) Synthesis and Evaluation of Bicyclic Hydroxypyridones as Inhibitors of Catechol O-Methyltransferase. ACS Med Chem Lett, 10, 1573–1578 DOI: 10.1021/acsmedchemlett.9b00345 [PubMed: 32038769]

Ferreira JJ, Lees A, Rocha JF, Poewe W, Rascol O & Soares-da-Silva P (2019) Long-term efficacy of opicapone in fluctuating Parkinson's disease patients: a pooled analysis of data from two phase 3 clinical trials and their open-label extensions. Eur J Neurol, 26, 953–960 DOI: 10.1111/ene.13914 [PubMed: 30681754]

Lachman HM, Papolos DF, Saito T, Yu YM, Szumlanski CL & Weinshilboum RM (1996) Human catechol-O-methyltransferase pharmacogenetics: description of a functional polymorphism and its potential application to neuropsychiatric disorders. Pharmacogenetics, 6, 243–250 DOI: 10.1097/00008571-199606000-00007 [PubMed: 8807664]

LeWitt PA (1993) Assessment of the dopaminergic lesion in Parkinson's disease by CSF markers. Adv Neurol, 60, 544–547 [PubMed: 8420188]

Magarkar A, Parkkila P, Viitala T, Lajunen T, Mobarak E, Licari G, Cramariuc O, Vauthey E, Rog T & Bunker A (2018) Membrane bound COMT isoform is an interfacial enzyme: general mechanism and new drug design paradigm. Chem Commun (Camb), 54, 3440–3443 DOI: 10.1039/c8cc00221e [PubMed: 29445781]

Mahat MY, Fakrudeen Ali Ahamed N, Chandrasekaran S, Rajagopal S, Narayanan S & Surendran N (2012) An improved method of transcutaneous cisterna magna puncture for cerebrospinal fluid sampling in rats. J Neurosci Methods, 211, 272–279 DOI: 10.1016/j.jneumeth.2012.09.013 [PubMed: 23000275]

Monk BC, Tomasiak TM, Keniya MV, Huschmann FU, Tyndall JD, O'Connell JD 3rd, Cannon RD, McDonald JG, Rodriguez A, Finer-Moore JS & Stroud RM (2014) Architecture of a single membrane spanning cytochrome P450 suggests constraints that orient the catalytic domain relative to a bilayer. Proc Natl Acad Sci U S A, 111, 3865–3870 DOI: 10.1073/pnas.1324245111 [PubMed: 24613931]

Nirogi R, Kandikere V, Mudigonda K, Bhyrapuneni G, Muddana N, Saralaya R & Benade V (2009) A simple and rapid method to collect the cerebrospinal fluid of rats and its application for the assessment of drug penetration into the central nervous system. J Neurosci Methods, 178, 116–119 DOI: 10.1016/j.jneumeth.2008.12.001 [PubMed: 19109998]

Parkkila P & Viitala T (2020) Partitioning of Catechol Derivatives in Lipid Membranes: Implications for Substrate Specificity to Catechol-O-methyltransferase. ACS Chem Neurosci DOI: 10.1021/acschemneuro.0c00049

Rivett AJ & Roth JA (1982) Kinetic studies on the O-methylation of dopamine by human brain membrane-bound catechol O-methyltransferase. Biochemistry, 21, 1740–1742 DOI: 10.1021/bi00537a006 [PubMed: 7082642]

Robinson RG, Smith SM, Wolkenberg SE, Kandebo M, Yao L, Gibson CR, Harrison ST, Polsky-Fisher S, Barrow JC, Manley PJ, Mulhearn JJ, Nanda KK, Schubert JW, Trotter BW, Zhao Z, Sanders JM, Smith RF, McLoughlin D, Sharma S, Hall DL, Walker TL, Kershner JL, Bhandari N, Hutson PH & Sachs NA (2012) Characterization of non-nitrocatechol pan and isoform specific catechol-O-methyltransferase inhibitors and substrates. ACS Chem Neurosci, 3, 129–140 DOI: 10.1021/cn200109w [PubMed: 22860182]

Roth JA (1992) Membrane-bound catechol-O-methyltransferase: a reevaluation of its role in the O-methylation of the catecholamine neurotransmitters. Rev Physiol Biochem Pharmacol, 120, 1–29 DOI: 10.1007/bfb0036121 [PubMed: 1519017]

Salamon A, Zadori D, Szpisjak L, Klivenyi P & Vecsei L (2019) Opicapone for the treatment of Parkinson's disease: an update. Expert Opin Pharmacother, 20, 2201–2207 DOI: 10.1080/14656566.2019.1681971 [PubMed: 31670988]

Tenhunen J (1996) Characterization of the rat catechol-O-methyltransferase gene proximal promoter: identification of a nuclear protein-DNA interaction that contributes to the tissue-specific regulation. DNA Cell Biol, 15, 461–473 DOI: 10.1089/dna.1996.15.461 [PubMed: 8672242]

Tenhunen J, Salminen M, Jalanko A, Ukkonen S & Ulmanen I (1993) Structure of the rat catechol-O-methyltransferase gene: separate promoters are used to produce mRNAs for soluble and membrane-bound forms of the enzyme. DNA Cell Biol, 12, 253–263 DOI: 10.1089/dna.1993.12.253 [PubMed: 8466648]

Tenhunen J, Salminen M, Lundstrom K, Kiviluoto T, Savolainen R & Ulmanen I (1994) Genomic organization of the human catechol O-methyltransferase gene and its expression from two distinct promoters. Eur J Biochem, 223, 1049–1059 DOI: 10.1111/j.1432-1033.1994.tb19083.x [PubMed: 8055944]

Ulmanen I, Peranen J, Tenhunen J, Tilgmann C, Karhunen T, Panula P, Bernasconi L, Aubry JP & Lundstrom K (1997) Expression and intracellular localization of catechol O-methyltransferase in transfected mammalian cells. Eur J Biochem, 243, 452–459 DOI: 10.1111/j.1432-1033.1997.0452a.x [PubMed: 9030772]

Westerink RH & Ewing AG (2008) The PC12 cell as model for neurosecretion. Acta Physiol (Oxf), 192, 273–285 DOI: 10.1111/j.1748-1716.2007.01805.x [PubMed: 18005394]

Zhang G, Buchler IP, DePasquale M, Wormald M, Liao G, Wei H, Barrow JC & Carr GV (2019) Development of a PC12 Cell Based Assay for Screening Catechol-O-methyltransferase Inhibitors. ACS Chem Neurosci, 10, 4221–4226 DOI: 10.1021/acschemneuro.9b00395 [PubMed: 31491076]

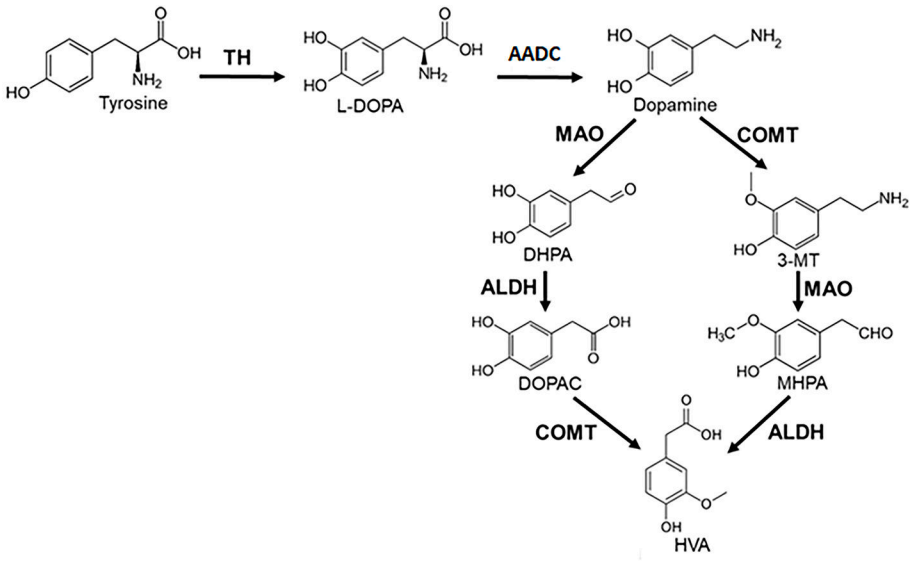

Fig. 1.
Schematic of dopamine metabolism.

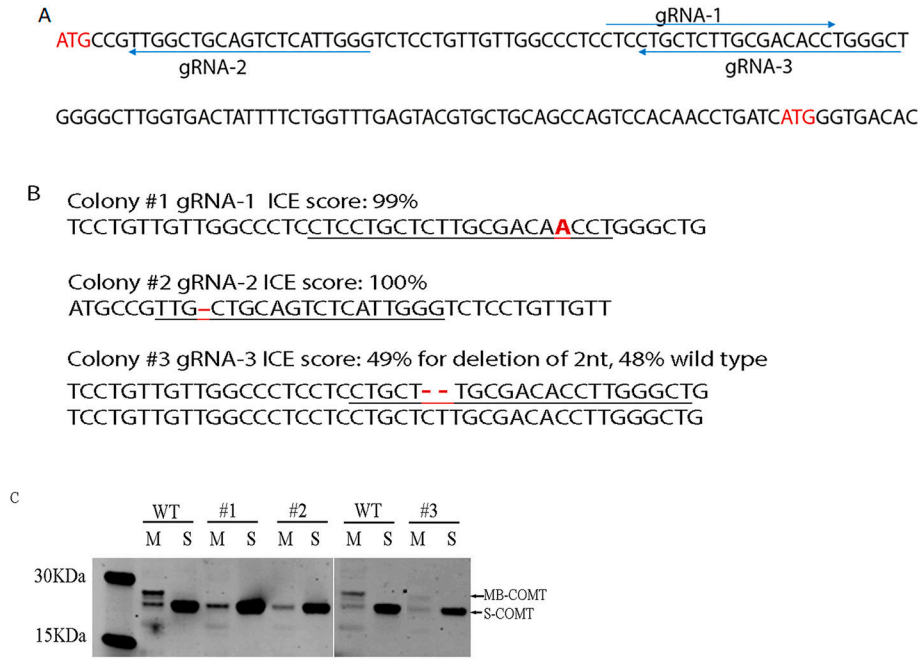

Fig. 2.

Knockout MB-COMT in PC12 cells using CRISPR-Cas9 technology. **A,** Genome sequence of rat COMT gene showing the region including two translational initiation codons for MB-COMT and S-COMT. Three guild RNAs (gRNAs) for MB-COMT knockout with corresponding sequences are either shaded or underlined. The arrows show the direction for each gRNA. **B**, Sequencing results for colony #1, #2 and #3. The Inference of **CRISPR** Edits (ICE) scores were calculated using the tool developed by Synthego (www.synthego.com). **C,** Western blots analysis for MB-COMT and S-COMT expression. Soluble (S) and membrane protein fractionation (M) were prepared as described. Proteins were analyzed with 4–20% SDS-PAGE and the expression of COMT proteins were detected by an antibody that recognizes both MB-COMT and S-COMT.

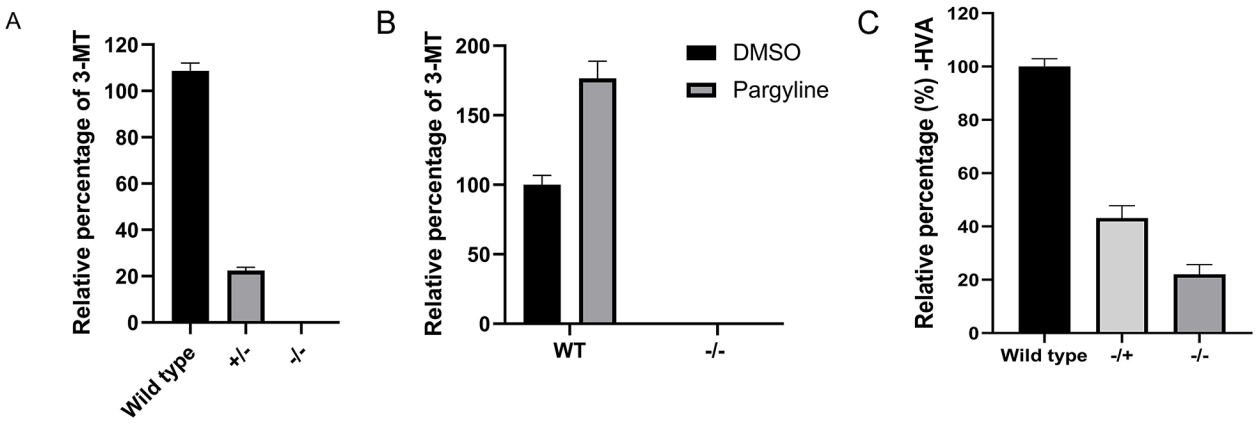

Fig. 3.

Effect of MB-COMT knockout on dopamine metabolism in PC12 cells. **A,** Relative level of 3-MT in PC12 cells with the heterozygous knockout (+/−) and complete knockout (−/−) of MB-COMT normalized to the level of 3-MT in the wild type PC12 cells (WT). **B,** Effect of pargyline on the level of 3-MT in wild type and MB-COMT knockout cells. Cells were treated with or without 0.1μM of pargyline, and the level of 3-MT was measured. The quantity of 3-MT was normalized to levels of 3-MT in wild type PC12 cells. **C,** Relative level of HVA in wild type, heterozygous and homozygous knockout of MB-COMT cells normalized to the amount of HVA in wild type cells. **D,** Relative level of DOPAC normalized to the amount of DOPAC in wild type PC12 cells.

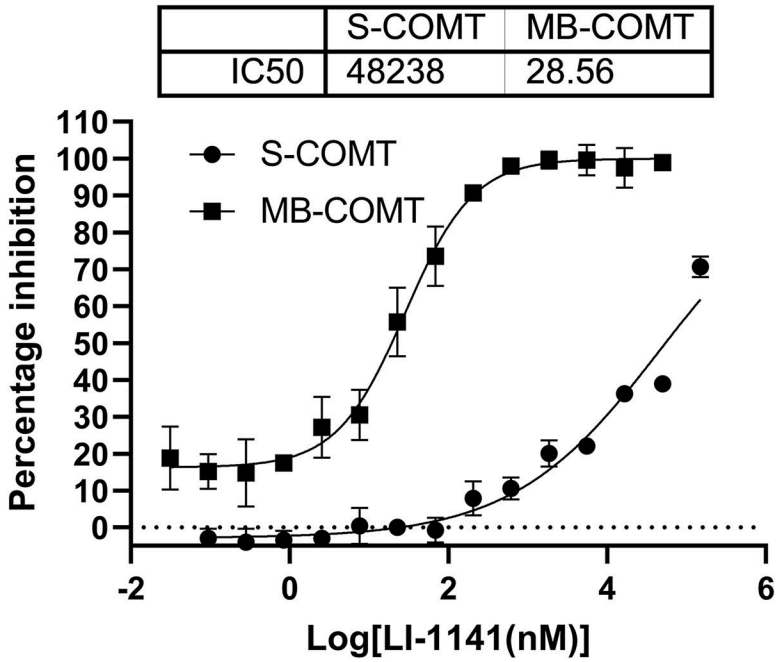

Fig. 4.

In vitro assay for dose-dependent inhibition of LI-1141 on MB-COMT and S-COMT. Fourteen doses of 3-fold dilution of LI-1141 were used to determine the IC_{50} of MB-COMT and S-COMT. The inhibition of tolcapone at 10 μM was used as 100% inhibition to calculate the percentage inhibition of LI-1141 at different concentrations. The dose-response curves and IC_{50}s were generated and calculated using Prism 9 software using a nonlinear regression model (4 parameters fit model).

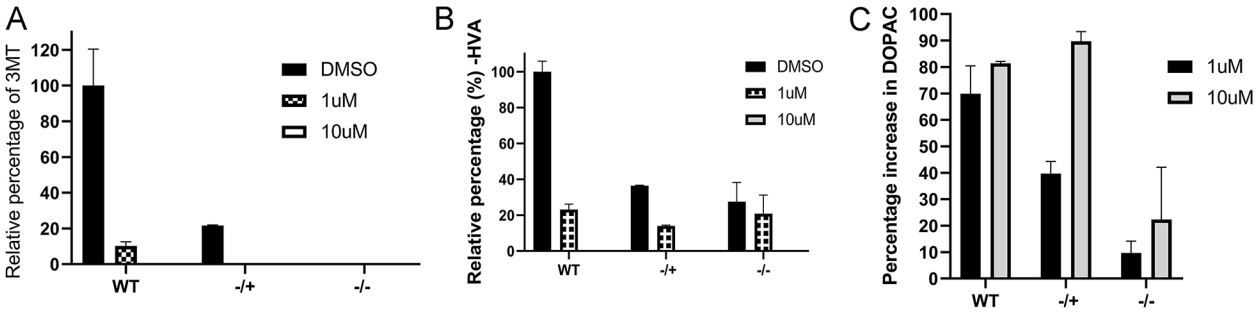

Fig. 5.

Effect of LI-1141 on dopamine metabolism in wild, heterozygous and homozygous deletion of MB-COMT cells. Wild type PC12 cells, heterozygous knockout (+/−) and complete knockout (−/−) of MB-COMT cells were treated with or without LI-1141. **A**, Relative level of 3-MT. The amount of the 3-MT was normalized to the level of 3-MT in the wild type PC12 cells. **B,** Relative level of HVA normalized to the HVA level in the wild type PC12 cells. **C**, The effect of the compound on the relative level of DOPAC. The percentage increase in DOPAC in each cell line was calculated by comparing to the level of DOPAC treated with LI-1141 to the cells treated with DMSO.

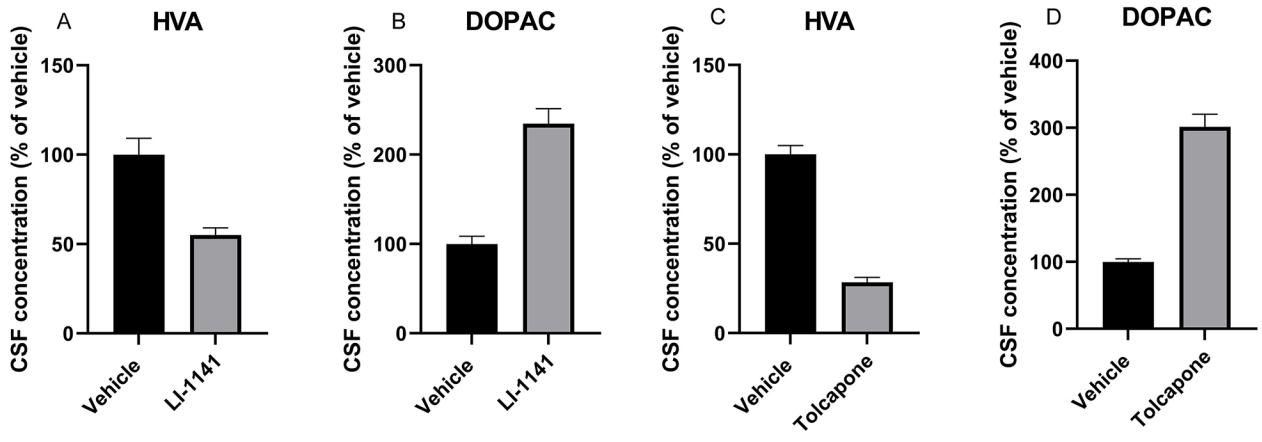

Fig. 6.

Effect of LI-1141 and tolcapone on HVA and DOPAC concentrations in CSF. Single doses of LI-1141 (100 mg/kg, PO) and tolcapone (15 mg/kg, IP) were administered four h before CSF sampling. The effect of each COMT inhibitor was compared to vehicle treatment. **A,** HVA concentration following LI-1141 or vehicle administration. **B,** DOPAC concentration following LI-1141 or vehicle administration. **C,** HVA concentration following tolcapone or vehicle administration. **D,** DOPAC concentration following tolcapone or vehicle administration. Data are normalized to the average of the vehicle treatment group and displayed as the mean + S.E.M. In the LI-1141 study, n = 6/vehicle and n = 7/LI-1141. In the tolcapone study, n = 7/vehicle and n = 8/tolcapone.